NASA/CR-2001-211237
ICASE Report No. 2001-33

Blending Methodology of Linear Parameter Varying Control Synthesis of F-16 Aircraft System

Jong-Yeob Shin
ICASE, Hampton, Virginia

Gary J. Balas
University of Minnesota, Minneapolis, Minnesota

Alpay M. Kaya
University of California, Berkeley, California

ICASE
NASA Langley Research Center
Hampton, Virginia
Operated by Universities Space Research Association

National Aeronautics and
Space Administration

Langley Research Center
Hampton, Virginia 23681-2199

Prepared for Langley Research Center
under Contract NAS1-97046

October 2001

Report Documentation Page

Report Date	Report Type	Dates Covered (from... to)
00OCT2001	N/A	-

Title and Subtitle Blending Methodology of Linear Parameter Varying Control Synthesis of F-16 Aircraft System	**Contract Number**
	Grant Number
	Program Element Number
Author(s) Gary J. Balas, Jong-Yeob Shin,Alpay M. Kaya	**Project Number**
	Task Number
	Work Unit Number
Performing Organization Name(s) and Address(es) National Aeronautics and Space Administration Langley Research Center Hampton, Virginia 23681-2199	**Performing Organization Report Number**
Sponsoring/Monitoring Agency Name(s) and Address(es)	**Sponsor/Monitor's Acronym(s)**
	Sponsor/Monitor's Report Number(s)

Distribution/Availability Statement
Approved for public release, distribution unlimited

Supplementary Notes
ICASE Report No. 2001-33

Abstract
Abstract: This paper presents the design of a linear parameter varying (LPV) controller for the F-16 longitudinal axes over the entire flight envelope using a blending methodology which lets an LPV controller preserve performance level over each parameter subspace and reduces computational costs for synthesizing an LPV controller. Three blending LPV controller synthesis methodologies are applied to control F-16 longitudinal axes. Using a function substitution method, a quasi-LPV model of the F-16 longitudinal axes is constructed from the nonlinear equations of motion over the entire flight envelope, including non-trim regions, to facilitate synthesis of LPV controllers for the F-16 aircraft. The nonlinear simulations of the blending LPV controller show that the desired performance and robustness objectives are achieved across all altitude variations.

Subject Terms

Report Classification unclassified	**Classification of this page** unclassified
Classification of Abstract unclassified	**Limitation of Abstract** SAR

Number of Pages
22

BLENDING METHODOLOGY OF LINEAR PARAMETER VARYING CONTROL SYNTHESIS OF F-16 AIRCRAFT SYSTEM

JONG-YEOB SHIN*, GARY J. BALAS†, AND ALPAY M. KAYA‡

Abstract. This paper presents the design of a linear parameter varying (LPV) controller for the F-16 longitudinal axes over the entire flight envelope using a blending methodology which lets an LPV controller preserve performance level over each parameter subspace and reduces computational costs for synthesizing an LPV controller. Three blending LPV controller synthesis methodologies are applied to control F-16 longitudinal axes. Using a function substitution method, a quasi-LPV model of the F-16 longitudinal axes is constructed from the nonlinear equations of motion over the entire flight envelope, including non-trim regions, to facilitate synthesis of LPV controllers for the F-16 aircraft. The nonlinear simulations of the blended LPV controller show that the desired performance and robustness objectives are achieved across all altitude variations.

Key words. LPV control synthesis, F-16 longitudinal axes

Subject classification. Guidance and Control

Nomenclature.

m, I_{yy}	:	Mass (slug), Inertial moments (slug ft^2)
V, $\overline{q}$	:	Velocity (ft sec^{-1}), Dynamic pressure (psi)
α, q	:	Angle of attack (rad), Pitch rate (rad sec^{-1})
θ, γ	:	Pitch angle (rad), Flight path angle (rad)
δ_e, T	:	Elevator deflection (rad), Thrust (lb)
$\bar{c}$, S	:	Chord length (ft), Reference area (ft^2)
X_{ac}, X_{cg}	:	Aerodynamic center position (ft), Center of gravity position (ft)
C_X, C_Z	:	X and Z force aerodynamic coefficients
C_{X_q}, C_{Z_q}	:	Aerodynamic stability derivatives
C_{m_o}	:	Pitch moment aerodynamic coefficient
Cm_q	:	Pitch moment aerodynamic stability derivative

1. Introduction. Extensive researches have focused over the last ten years on developing analysis and synthesis techniques for gain-scheduled controllers for linear parameter varying (LPV) systems [13, 12, 17, 6, 2, 15]. In Ref. [13, 12], conditions are given which guarantee stability, robustness, and performance properties of the global gain-scheduled designs. Recent theoretical developments have produced methods for synthesizing gain-scheduling controllers for LPV systems, which guarantee a level of robust stability and performance across scheduling parameter spaces [6, 2, 15]. In Ref. [2], LPV control synthesis methods have also been developed using parameter-dependent Lyapunov functions to lead to a less conservative result. This gain-scheduling approach has been successfully applied to synthesize controllers for pitch-axis

*ICASE, MS 132C, NASA Langley Research Center, Hampton, VA 23681. This research was supportd by National Aeronautics and Space Administration under NASA Contract No. NAS1-97046 while the first author was in residence at ICASE, NASA Langley Research Center, Hampton, VA 23681.

†Professor, Department of Aerospace Engineering and Mechanics, University of Minnesota, 110 Union St. SE, Minneapolis, MN 55455.

‡Graduate Research Assistant, Department of Mechanical Engineering, University of California, Berkeley, CA 94720.

missile autopilots [3, 11], F-14 aircraft lateral-directional axis during powered approach [4, 5], and turbofan engines [8].

One of the potential difficulties in practical uses of the LPV synthesis methodology with parameter-dependent Lyapunov functions is that the complexity of the linear matrix inequality (LMI) optimization problem increases exponentially with the number of scheduling parameters and the number of the grid points over the scheduling parameter spaces. One approach to facilitate practical use of LPV synthesis methodology, denoted as the "blending approach", has been discussed in Ref. [15, 14]. This approach to control design partitions the full parameter space into overlapping small subspaces. An LPV controller is synthesized for each small region. These regional controllers are blended into a single LPV controller for the entire parameter space. In this paper, this blending approach is applied to control F-16 longitudinal axes over the entire flight envelope.

To synthesize an LPV controller for an F-16 aircraft, an LPV model of the aircraft dynamics is required. Conventional approaches to generate an LPV model of an aircraft are based on Jacobian linearizations at trim points or a change of state coordinates [11] to reduce the nonlinearity of aircraft dynamics. The LPV models constructed by both approaches can present aircraft dynamics at trim conditions. However, the models can not represent aircraft dynamics at non-trim conditions. Instead of using Jacobian linearization or state transformation, the nonlinear terms of aircraft dynamics can be substituted for other functions in quasi-LPV form [18, 19]. This function substitution approach can be applied for both trim and non-trim conditions. The approach has been used in generating a quasi-LPV model of a generic missile [18, 19]. In this paper, a quasi-LPV model of F-16 longitudinal axes is provided over the entire flight envelope including non-trim regions, using a function substitution approach.

In Section 2, a brief summary of conventional LPV controller synthesis used in this paper is presented to emphasize the complexity of the LMI optimizations. In Section 3, three blending LPV control synthesis methodologies are presented. Development of a quasi-LPV model of F-16 longitudinal axes is presented in Section 4. In Section 5, formulation of the LPV control problem and the blending of two LPV controllers of the F-16 aircraft are presented. Nonlinear simulations of the closed-loop system with the blended controller are presented in Section 6 and this paper concludes with a brief summary in Section 7.

2. LPV Control Synthesis. In this section, a conventional LPV control synthesis using parameter-dependent Lyapunov functions[2] is briefly described. Consider a generalized linear open-loop system as functions of parameters $\rho(t) \in \mathcal{P}$. For a compact subset $\mathcal{P} \subset \mathcal{R}^s$, the parameter variation set denotes the set of all piecewise continuous functions mapping R (time) into $\mathcal{P}$ with a finite number of discontinuities in any interval, where s is the number of parameters. An LPV open-loop system can be written as

$$\begin{bmatrix} \dot{x}(t) \\ e(t) \\ y(t) \end{bmatrix} = \begin{bmatrix} A(\rho(t)) & B_1(\rho(t)) & B_2(\rho(t)) \\ C_1(\rho(t)) & 0 & D_{12}(\rho(t)) \\ C_2(\rho(t)) & D_{21}(\rho(t)) & 0 \end{bmatrix} \begin{bmatrix} x(t) \\ d(t) \\ u(t) \end{bmatrix}, \tag{2.1}$$

where $y(t)$, $e(t)$, $d(t)$ and $u(t)$ are measurements, errors, disturbances, and control signals. Hereafter, ρ denotes $\rho(t)$. The induced $\mathcal{L}_2$ norm of d to e is defined as

$$\sup_{\rho \in \mathcal{P}, d \in \mathcal{L}_2, ||d||_2 \neq 0} \frac{||e||_2}{||d||_2}.$$

In a conventional LPV synthesis methodology, suppose there is an LPV output feedback controller $K(\rho)$ which stabilizes the closed-loop system exponentially and makes the induced $\mathcal{L}_2$-norm of d to e less than γ.

The controller $K(\rho)$ can be written as

$$\begin{bmatrix} \dot{x}_k \\ u \end{bmatrix} = \begin{bmatrix} A_k(\rho) & B_k(\rho) \\ C_k(\rho) & D_k(\rho) \end{bmatrix} \begin{bmatrix} x_k \\ y \end{bmatrix}. \tag{2.2}$$

An LPV controller $K(\rho)$ can be constructed from solutions of $X(\rho)$ and $Y(\rho)$ of the following optimization problem [2]:

$$\min_{X,Y \in \mathcal{R}^{n \times n}} \gamma \tag{2.3}$$

subject to

$$\begin{bmatrix} X(\rho)\hat{A}^T(\rho) + \hat{A}(\rho)X(\rho) - \sum_{i=1}^{s}(\underline{\nu}_i \frac{\partial X}{\partial \rho_i}) - B_2(\rho)B_2^T(\rho) & X(\rho)C_{11}^T(\rho) & \gamma^{-1}B_1(\rho) \\ C_{11}(\rho)X(\rho) & -I_{n_{e_1}} & 0 \\ \gamma^{-1}B_1^T(\rho) & 0 & -I_{n_d} \end{bmatrix} < 0, \tag{2.4}$$

$$\begin{bmatrix} \tilde{A}(\rho)Y(\rho) + Y(\rho)\tilde{A}^T(\rho) + \sum_{i=1}^{s}(\underline{\nu}_i \frac{\partial Y}{\partial \rho_i}) - C_2^T(\rho)C_2(\rho) & Y(\rho)B_{11}(\rho) & \gamma^{-1}C_1^T(\rho) \\ B_{11}^T(\rho)Y(\rho) & -I_{n_{d_1}} & 0 \\ \gamma^{-1}C_1(\rho) & 0 & -I_{n_e} \end{bmatrix} < 0, \tag{2.5}$$

$$\begin{bmatrix} X(\rho) & \gamma^{-1}I_n \\ \gamma^{-1}I_n & Y(\rho) \end{bmatrix} \geq 0, \tag{2.6}$$

$$X(\rho) > 0, \;\; Y(\rho) > 0,$$

where

$$\hat{A}(\rho) \equiv A(\rho) - B_2(\rho)C_{12}(\rho), \;\; \tilde{A}(\rho) \equiv A(\rho) - B_{12}(\rho)C_2(\rho), \tag{2.7}$$

and n is the number of states of the generalized open-loop system. The detailed definitions of matrices $C_{11}(\rho)$, $C_{12}(\rho)$, and $B_{11}(\rho)$ can be found in Ref. [2]. Note that $\sum_{i=1}^{s} \underline{\nu}_i$ indicates that every combination of $\underline{\nu}_i$ and $\bar{\nu}_i$ is included in the LMIs. The parameter rate $\dot{\rho}$ is bounded as $\underline{\nu}_i \leq \dot{\rho}_i \leq \bar{\nu}_i$.

A method to construct an LPV controller $K(\rho)$ from the solutions $X(\rho)$ and $Y(\rho)$ is taken from Ref. [2]. In this paper, an LPV controller is constructed as [2]:

$$A_k(\rho) = A(\rho) + B_2(\rho)F(\rho) + Q^{-1}(\rho)Y(\rho)L(\rho)C_2(\rho) - \gamma^{-2}Q^{-1}(\rho)M(\rho,\dot{\rho}), \tag{2.8}$$

$$B_k(\rho) = -Q^{-1}(\rho)Y(\rho)L(\rho), \tag{2.9}$$

$$C_k(\rho) = F(\rho), \tag{2.10}$$

$$D_k(\rho) = 0, \tag{2.11}$$

where matrices $Q(\rho)$, $F(\rho)$, $L(\rho)$, and $M(\rho,\dot{\rho})$ are defined as

$$\begin{aligned} Q(\rho) &= Y(\rho) - \gamma^{-2}X^{-1}(\rho), \\ F(\rho) &= -[B_2^T(\rho)X^{-1}(\rho) + D_{12}^T(\rho)C_1(\rho)], \\ L(\rho) &= -[Y^{-1}(\rho)C_2^T(\rho) + B_1(\rho)D_{21}^T(\rho)], \\ M(\rho,\dot{\rho}) &= H(\rho,\dot{\rho}) + \gamma^2 Q(\rho)[-Q^{-1}(\rho)Y(\rho)L(\rho)D_{21}(\rho) - B_1(\rho)]B_1^T(\rho)X^{-1}(\rho). \end{aligned}$$

Matrix $H(\rho, \dot{\rho})$ is defined as

$$H(\rho,\dot{\rho}) = -\left[X^{-1}(\rho)A_F(\rho) + A_F(\rho)^T X^{-1}(\rho) + \sum_{i=1}^{s}\left(\dot{\rho}_i \frac{\partial X^{-1}}{\partial \rho_i}\right)\right.$$
$$\left. + C_F^T(\rho)C_F(\rho) + \gamma^{-2}X^{-1}(\rho)B_1(\rho)B_1(\rho)^T X^{-1}(\rho)\right]$$

with $A_F(\rho) = A(\rho)+B_2(\rho)F(\rho)$ and $C_F(\rho) = C_1(\rho)+D_{12}(\rho)F(\rho)$. The closed-loop system with the controller $K(\rho)$ is exponentially stable and the induced $\mathcal{L}_2$ norm is less than γ. The proof can be found in Ref. [2].

To make the optimization problem of equation (2.3) computationally tractable, the scheduling parameters ρ are discretized into grid points. Thus, an infinite number of constraints are represented by a finite number of LMI constraints. Also, $X(\rho)$ and $Y(\rho)$ are represented by a finite number of basis functions $h_i(\rho)$ and $g_i(\rho)$:

$$X(\rho) = \sum_{i=1}^{N_x} h_i(\rho)X_i, \quad Y(\rho) = \sum_{i=1}^{N_y} g_i(\rho)Y_i,$$

where $h_i(\rho)$ and $g_i(\rho)$ are continuously differentiable functions. The LMIs of equations (2.4)-(2.6) are solved for all grid points of the scheduling parameters simultaneously. The size of the optimization problem is proportional to $2^{s+1}N_g$ where s and N_g are the number of scheduling parameters and total number of grid points over the scheduling parameter space. The number of decision variables are $(N_x + N_y)\frac{n(n+1)}{2}$, where N_x, N_y and n are the order of basis functions of X and Y, and the state order. Thus, computational time to solve the optimization problem of equation (2.3) is dependent on the number of grid points of scheduling parameters, the state order of a generalized open-loop system, and basis function orders. The conventional LPV synthesis methodology may require expensive computational cost (computational time and computer memory) when number of scheduling parameters increases. In the next section, a blending method to reduce the computational cost to synthesize an LPV controller and to preserve performance level over parameter subspaces is presented.

3. LPV Controller Blending Approach. Instead of designing a single LPV controller for the entire parameter set in a conventional LPV synthesis, LPV controllers can be synthesized for parameter subsets, which are overlapped with each other. Then, these LPV controllers are blended into a single LPV controller over the entire parameter set. Thus, the performance of the closed-loop system with the blended controller is preserved when parameter trajectories travel over the overlapped parameter subsets.

Consider the scheduling parameter vector $\rho \in \mathcal{P}$ which consists of subvectors $\rho_s \in \mathcal{P}_s$ and $\rho_d \in \mathcal{P}_d$. The parameter subset $\mathcal{P}_s$ can be partitioned into two subsets with the following conditions:

$$\mathcal{P}_{s_\cap} = \mathcal{P}_{s_1} \cap \mathcal{P}_{s_2}, \tag{3.1}$$
$$\mathcal{P}_s = \mathcal{P}_{s_1} \cup \mathcal{P}_{s_2}. \tag{3.2}$$

Suppose that there exist LPV controllers K_1 and K_2 constructed from parameter-dependent Lyapunov functions of a parameter subvector ρ_d, over each parameter subset $\mathcal{P}_{s_i} \cup \mathcal{P}_d$, $i = 1, \quad 2$. Thus, X_i and Y_i are functions of ρ_d (not ρ_s) over each parameter subset $\mathcal{P}_{s_i} \cup \mathcal{P}_d, i = 1, \quad 2$. Also, the controller K_i can stabilize the closed-loop system and the induced-$\mathcal{L}_2$ norm of the closed-loop system is less than γ_i over each parameter subset $\mathcal{P}_{s_i} \cup \mathcal{P}_d$.

When a scheduling parameter subvector ρ_s is in the intersection subset $\mathcal{P}_{s_\cap}$, LMI solution matrices $X_i(\rho_d)$ and $Y_i(\rho_d)$ are combined into $X_b(\rho_s, \rho_d)$ and $Y_b(\rho_s, \rho_d)$, respectively. There are three methods to

calculate $X_b(\rho_s, \rho_d)$ and $Y_b(\rho_s, \rho_d)$, which will be explained later. The blended matrices $X_b(\rho_s, \rho_d)$ and $Y_b(\rho_s, \rho_d)$ should be feasible solutions of the LMI constraints of equations (2.4)-(2.5) over the parameter subset $\mathcal{P}_{s_\cap} \cup \mathcal{P}_d$. When the parameter subvector ρ_s is in the parameter subset $\mathcal{P}_{s_i} - \mathcal{P}_{s_\cap}$, $X_b(\rho_s, \rho_d)$ and $Y_b(\rho_s, \rho_d)$ should be equal to $X_i(\rho_d)$ and $Y_i(\rho_d)$, respectively, and the partial derivatives of $\frac{\partial X_b}{\partial \rho}$ and $\frac{\partial Y_b}{\partial \rho}$ should be equal to $\frac{\partial X_i}{\partial \rho}$ and $\frac{\partial Y_i}{\partial \rho}$, respectively. There are three blending methods for X_b and Y_b to satisfy the feasibility condition and the boundary conditions.

For method I, matrices $X_b(\rho_s, \rho_d)$ and $Y_b(\rho_s, \rho_d)$ can be written as:

$$X_b(\rho_s, \rho_d) = \sum_{i=1}^{2} b_{x_i}(\rho_s) X_i(\rho_d), \tag{3.3}$$

$$Y_b(\rho_s, \rho_d) = \sum_{i=1}^{2} b_{y_i}(\rho_s) Y_i(\rho_d), \tag{3.4}$$

where "blending functions" $b_{x_i}(\rho_s)$ and $b_{y_i}(\rho_s)$ are differentiable scalar functions. To satisfy the boundary conditions of X_b and Y_b, blending functions $b_{x_i}(\rho_s)$ and $b_{y_i}(\rho_s)$ are defined as:

$$b_{x_i}(\rho_s) = \begin{cases} 1, & \rho_s \in \mathcal{P}_{s_i} - \mathcal{P}_{s_\cap}, \\ 0, & \rho_s \in \mathcal{P}_s - \mathcal{P}_{s_i}, \end{cases} \tag{3.5}$$

$$b_{y_i}(\rho_s) = \begin{cases} 1, & \rho_s \in \mathcal{P}_{s_i} - \mathcal{P}_{s_\cap}, \\ 0, & \rho_s \in \mathcal{P}_s - \mathcal{P}_{s_i}, \end{cases} \tag{3.6}$$

$$\frac{\partial b_{x_i}(\rho_s)}{\partial \rho_s} = 0, \qquad \frac{\partial b_{y_i}(\rho_s)}{\partial \rho_s} = 0, \qquad \rho_s \in \mathcal{P}_{s_i} - \mathcal{P}_{s_\cap}. \tag{3.7}$$

Suppose that the blending functions $b_{x_i}(\rho_s)$ and $b_{y_i}(\rho_s)$ satisfy the following conditions:

$$\sum_{i=1}^{2} b_{x_i}(\rho_s) = 1, \quad 0 \le b_{x_i}(\rho_s) \le 1, \quad \rho_s \in \mathcal{P}_{s_\cap}, \tag{3.8}$$

$$\sum_{i=1}^{2} b_{y_i}(\rho_s) = 1, \quad 0 \le b_{y_i}(\rho_s) \le 1, \quad \rho_s \in \mathcal{P}_{s_\cap}, \tag{3.9}$$

and γ is chosen as $\max(\gamma_1, \gamma_2)$. Then, the following equations are satisfied, since the LMIs of equations (2.4)-(2.5) are convex with respect to X and Y. Hereafter, ρ dependence is omitted for convenience.

$$X_b \hat{A}^T + \hat{A} X_b - \sum_{i=1}^{s} (\underline{\bar{\nu}}_i \sum_{j=1}^{2} b_{x_j} \frac{\partial X_j}{\partial \rho_i}) - B_2 B_2^T + X_b C_{11}^T C_{11} X_b + \gamma^{-2} B_1 B_1^T < 0, \tag{3.10}$$

$$\tilde{A} Y_b \; + Y_b \tilde{A}^T \; + \sum_{i=1}^{s} (\underline{\bar{\nu}}_i \sum_{j=1}^{2} b_{y_j} \frac{\partial Y_j}{\partial \rho_i}) \; - C_2^T C_2 + Y_b B_{11} B_{11}^T Y_b \; + \gamma^{-2} C_1^T C_1 < 0. \tag{3.11}$$

When the derivatives of blending functions $\frac{\partial b_{x_i}(\rho_s)}{\partial \rho_s}$ and $\frac{\partial b_{y_i}(\rho_s)}{\partial \rho_s}$ are small enough to satisfy the following inequalities,

$$\bar{\sigma} \left(\sum_{i=1}^{s} \left\{ \underline{\bar{\nu}}_i \sum_{j=1}^{2} X_j(\rho) \frac{\partial b_{x_j}(\rho_s)}{\partial \rho_i} \right\} \right) < \underline{\sigma}(M_X), \tag{3.12}$$

$$\bar{\sigma} \left(\sum_{i=1}^{s} \left\{ \underline{\bar{\nu}}_i \sum_{j=1}^{2} Y_j(\rho) \frac{\partial b_{y_j}(\rho_s)}{\partial \rho_i} \right\} \right) < \underline{\sigma}(M_Y), \tag{3.13}$$

it is obviously noted that the blended $X_b(\rho_s, \rho_d)$ and $Y_b(\rho_s, \rho_d)$ can be feasible solutions of LMIs of equations (2.4)-(2.6) over the parameter subset $\mathcal{P}_{s_\cap}$, where matrices M_X and M_Y are defined as

$$M_X \equiv X_b\hat{A}^T + \hat{A}X_b - \sum_{i=1}^{s}(\underline{\bar{\nu}}_i \sum_{j=1}^{2} b_{x_j}\frac{\partial X_j}{\partial \rho_i}) - B_2B_2^T + X_bC_{11}^TC_{11}X_b + \gamma^{-2}B_1B_1^T,$$

$$M_Y \equiv \tilde{A}Y_b + Y_b\tilde{A}^T + \sum_{i=1}^{s}(\underline{\bar{\nu}}_i \sum_{j=1}^{2} b_{y_j}\frac{\partial Y_j}{\partial \rho_i}) - C_2^TC_2 + Y_bB_{11}B_{11}^TY_b + \gamma^{-2}C_1^TC_1.$$

Here, $\bar{\sigma}$ and $\underline{\sigma}$ represent the maximum and the minimum singular values, respectively.

The procedure of designing an LPV controller over the entire parameter set using this blending method I is:

1. Partition the entire parameter set into two subsets which have the overlapped subset.
2. Solve the LMI optimization of equation (2.3) for $X_i(\rho_d)$ and $Y_i(\rho_d)$ over each parameter subset.
3. Define blending scalar functions $b_{x_i}(\rho_s)$ and $b_{y_i}(\rho_s)$ which satisfy the boundary conditions of equations (3.5)-(3.7) and the derivative conditions of equations (3.12)-(3.13). Note that the derivative conditions are sufficient for $X_b(\rho_s, \rho_d)$ and $Y_b(\rho_s, \rho_d)$ to be feasible solutions of the LMI constraints of equations (2.4)-(2.5) over the parameter subset $\mathcal{P}_{s_\cap} \cup \mathcal{P}_d$. A controller designer chooses candidate blending functions until the feasibility conditions of equations (2.4)-(2.5) are satisfied.
4. Construct an LPV controller over the entire parameter set $\mathcal{P}_s \cup \mathcal{P}_d$ using equations (2.8)-(2.11), from the calculated X_b and Y_b of equations (3.3)-(3.4).

For method II, an alternative way to calculate the blended matrices $X(\rho_s, \rho_d)$ and $Y(\rho_s, \rho_d)$ as feasible solutions of the LMIs of equations (2.4)-(2.6) is adding extra LMIs in conventional LPV synthesis with candidate blending functions [2]. The extra LMIs are:

$$\begin{bmatrix} \sum_{j=1}^{2} b_{x_j}X_j\hat{A}^T + \hat{A}\sum_{j=1}^{2} b_{x_j}X_j + \sum_{i=1}^{s}(\underline{\bar{\nu}}_i\frac{\partial}{\partial\rho_i}\sum_{j=1}^{2} b_{x_j}X_j) - B_2B_2^T & \sum_{j=1}^{2} b_{x_j}X_jC_{11}^T & \gamma^{-1}B_1 \\ C_{11}\sum_{j=1}^{2} b_{x_j}X_j & -I_{n_{e_1}} & 0 \\ \gamma^{-1}B_1^T & 0 & -I_{n_d} \end{bmatrix} < 0, \tag{3.14}$$

$$\begin{bmatrix} \tilde{A}\sum_{j=1}^{2} b_{y_j}Y_j + \sum_{j=1}^{2} b_{y_j}Y_j\tilde{A}^T + \sum_{i=1}^{s}(\underline{\bar{\nu}}_i\frac{\partial}{\partial\rho_i}\sum_{j=1}^{2} b_{y_j}Y_j) - C_2^TC_2 & \sum_{j=1}^{2} b_{y_j}Y_jB_{11} & \gamma^{-1}C_1^T \\ B_{11}^T\sum_{j=1}^{2} b_{y_j}Y_j & -I_{n_{d_1}} & 0 \\ \gamma^{-1}C_1 & 0 & -I_{n_e} \end{bmatrix} < 0. \tag{3.15}$$

The procedure of designing an LPV controller over the entire parameter set using this blending method II is:

1. Partition the entire parameter set into two subsets which have the overlapped subset.
2. Solve the LMI optimization of equation (2.3) for the solution matrices $X_1(\rho_d)$ and $Y_1(\rho_d)$ over one of parameter subsets, which is denoted by $\mathcal{P}_{s_1} \cup \mathcal{P}_d$.
3. Define blending scalar functions $b_{x_i}(\rho_s)$ and $b_{y_i}(\rho_s)$ which satisfy the boundary conditions of equations (3.5)-(3.7).

4. Solve the LMI optimization problem of equation (2.3) with the extra LMI constraints of equations (3.14)-(3.15) for the solution matrices $X_2(\rho_d)$ and $Y_2(\rho_d)$ over the other parameter subset $\mathcal{P}_{s_2} \cup \mathcal{P}_d$.
5. Construct an LPV controller over the entire parameter set using equations (2.8)-(2.11) with the X_b and Y_b calculated using equations (3.3)-(3.4).

The LMI optimization over the second parameter subset $\mathcal{P}_{s_2} \cup \mathcal{P}_d$ is related with the solution matrices X_1 and Y_1 over the first parameter subset $\mathcal{P}_{s_1} \cup \mathcal{P}_d$. Thus, defining the order of parameter subsets may affect the designed LPV controller over the entire parameter set.

Both methods I and II require appropriate blending functions to blend solution matrices over the parameter subset $\mathcal{P}_{s_\cap}$. Note that an LPV controller provided by the blending methods I and II changes dependently on which blending functions are selected. It is unknown how this affects the closed-loop performance of the designed LPV controller.

For method III, blending matrix functions are calculated to minimize the induced $\mathcal{L}_2$ norm γ over the parameter subset $\mathcal{P}_{s_\cap} \cup \mathcal{P}_d$. The blended solution matrices X_b and Y_b are rewritten as:

$$X_b(\rho_s, \rho_d) = \frac{1}{2}[X_{b_1}(\rho_s)X_1(\rho_d) + X_1(\rho_d)X_{b_1}(\rho_s)] + \frac{1}{2}[X_{b_2}(\rho_s)X_2(\rho_d) + X_2(\rho_d)X_{b_2}(\rho_s)], \tag{3.16}$$

$$Y_b(\rho_s, \rho_d) = \frac{1}{2}[Y_{b_1}(\rho_s)Y_1(\rho_d) \;\; + \;\; Y_1(\rho_d)Y_{b_1}(\rho_s)] + \frac{1}{2}[Y_{b_2}(\rho_s)Y_2(\rho_d) \;\; + \;\; Y_2(\rho_d)Y_{b_2}(\rho_s)], \tag{3.17}$$

where "blending matrix functions" $X_{b_1}(\rho_s)$, $X_{b_2}(\rho_s)$, $Y_{b_1}(\rho_s)$, and $Y_{b_2}(\rho_s)$ are differentiable symmetric matrix functions bounded over the parameter subset $\mathcal{P}_{s_\cap}$. To present the blending matrix functions, basis functions $g_{x_j}(\rho_s)$, $h_{x_j}(\rho_s)$, $g_{y_j}(\rho_s)$, and $h_{y_j}(\rho_s)$ for $X_{b_1}(\rho_s)$, $X_{b_2}(\rho_s)$, $Y_{b_1}(\rho_s)$, and $Y_{b_2}(\rho_s)$ are introduced, respectively. To satisfy the boundary condition of blended matrices $X_b(\rho_s, \rho_d)$ and $Y_b(\rho_s, \rho_d)$, $X_{b_1}(\rho_s)$, $X_{b_2}(\rho_s)$, $Y_{b_1}(\rho_s)$, and $Y_{b_2}(\rho_s)$ are defined as:

$$X_{b_1}(\rho_s) = g_{x_0}(\rho_s)I + \sum_{j=1}^{N_{xg}} g_{x_j}(\rho_s)X_{b_{1_j}}, \quad X_{b_2}(\rho_s) = h_{x_0}(\rho_s)I + \sum_{j=1}^{N_{xh}} h_{x_j}(\rho_s)X_{b_{2_j}}, \tag{3.18}$$

$$Y_{b_1}(\rho_s) = g_{y_0}(\rho_s)I + \sum_{j=1}^{N_{yg}} g_{y_j}(\rho_s)Y_{b_{1_j}}, \quad Y_{b_2}(\rho_s) = h_{y_0}(\rho_s)I + \sum_{j=1}^{N_{yh}} h_{y_j}(\rho_s)Y_{b_{2_j}}, \tag{3.19}$$

where

$$\begin{aligned}
&g_{x_0}(\rho_s) = 1, \quad h_{x_j}(\rho_s) = 0, \quad \frac{\partial g_{x_j}(\rho_s)}{\partial \rho_{s_i}} = \frac{\partial h_{x_j}(\rho_s)}{\partial \rho_{s_i}} = 0, \quad \rho_s \in \mathcal{P}_{s_1} - \mathcal{P}_{s_\cap}, \\
&h_{x_0}(\rho_s) = 1, \quad g_{x_j}(\rho_s) = 0, \quad \frac{\partial g_{x_j}(\rho_s)}{\partial \rho_{s_i}} = \frac{\partial h_{x_j}(\rho_s)}{\partial \rho_{s_i}} = 0, \quad \rho_s \in \mathcal{P}_{s_2} - \mathcal{P}_{s_\cap}, \\
&g_{y_0}(\rho_s) = 1, \quad h_{y_j}(\rho_s) = 0, \quad \frac{\partial g_{y_j}(\rho_s)}{\partial \rho_{s_i}} = \frac{\partial h_{y_j}(\rho_s)}{\partial \rho_{s_i}} = 0, \quad \rho_s \in \mathcal{P}_{s_1} - \mathcal{P}_{s_\cap}, \\
&h_{y_0}(\rho_s) = 1, \quad g_{y_j}(\rho_s) = 0, \quad \frac{\partial g_{y_j}(\rho_s)}{\partial \rho_{s_i}} = \frac{\partial h_{y_j}(\rho_s)}{\partial \rho_{s_i}} = 0, \quad \rho_s \in \mathcal{P}_{s_2} - \mathcal{P}_{s_\cap}.
\end{aligned} \tag{3.20}$$

Here, the basis functions are differentiable over the parameter subset $\mathcal{P}_{s_\cap}$ and $X_{b_{1_j}}$, $X_{b_{2_j}}$, $Y_{b_{1_j}}$, and $Y_{b_{2_j}}$ are unknown constant matrices in $\mathcal{R}^{n \times n}$. The unknown constant matrices can be determined solving the following LMI optimization:

$$\min_{X_{b_{1_j}}, X_{b_{2_j}}, Y_{b_{1_j}}, Y_{b_{2_j}} \in \mathcal{R}^{n \times n}} \gamma, \tag{3.21}$$

$$\begin{bmatrix} X_b\hat{A}^T + \hat{A}X_b - \sum_{i=1}^{s}(\underline{\nu}_i \frac{\partial X_b}{\partial \rho_i}) - B_2B_2^T & X_bC_{11}^T & \gamma^{-1}B_1 \\ C_{11}X_b & -I_{n_{e_1}} & 0 \\ \gamma^{-1}B_1^T & 0 & -I_{n_d} \end{bmatrix} < 0, \tag{3.22}$$

$$\begin{bmatrix} \tilde{A}Y_b + Y_b\tilde{A}^T + \sum_{i=1}^{s}(\underline{\nu}_i \frac{\partial Y_b}{\partial \rho_i}) - C_2^TC_2 & Y_bB_{11} & \gamma^{-1}C_1^T \\ B_{11}^TY_b & -I_{n_{d_1}} & 0 \\ \gamma^{-1}C_1 & 0 & -I_{n_e} \end{bmatrix} < 0, \tag{3.23}$$

$$\begin{bmatrix} X_b & \gamma^{-1}I_n \\ \gamma^{-1}I_n & Y_b \end{bmatrix} \geq 0, \quad X_b > 0, \quad Y_b > 0, \tag{3.24}$$

where

$$\begin{aligned} X_b &= g_{x_0}X_1 + h_{x_0}X_2 + 0.5\left\{\sum_{j=1}^{N_{x_g}} g_{x_j}[X_1X_{b_{1_j}} + X_{b_{1_j}}X_1] + \sum_{k=1}^{N_{x_h}} h_{x_k}[X_2X_{b_{2_k}} + X_{b_{2_k}}X_2]\right\}, \\ Y_b &= g_{y_0}Y_1 + h_{y_0}Y_2 + 0.5\left\{\sum_{j=1}^{N_{y_g}} g_{y_j}[\,Y_1Y_{b_{1_j}} + Y_{b_{1_j}}Y_1\,] + \sum_{k=1}^{N_{y_h}} h_{y_k}[Y_2Y_{b_{2_k}} + Y_{b_{2_k}}Y_2]\right\}. \end{aligned} \tag{3.25}$$

The procedure of designing an LPV controller over the entire parameter set using this blending method III is:

1. Partition the entire parameter set into two subsets which have the overlapped subset.
2. Solve the LMI optimization of equation (2.3) for $X_i(\rho)$ and $Y_i(\rho)$ over each parameter subset.
3. Define basis functions for blending matrix functions in equations (3.18) and (3.19), which satisfy the boundary conditions of equation (3.20) over each parameter subset.
4. Solve the LMI optimization of equation (3.21) over the parameter subset $\mathcal{P}_{s_\cap} \cup \mathcal{P}_d$.
5. Construct solution matrices X and Y over the entire parameter set using the solution matrices X_1, X_2, Y_1, Y_2, X_b, and Y_b.
6. Construct an LPV controller over the entire parameter set using equations (2.8)-(2.11) based on solution matrices X and Y generated in step 5.

In this section, there were described three methods to calculate the blended solution matrices $X_b(\rho_s, \rho_d)$ and $Y_b(\rho_s, \rho_d)$ which are feasible solutions of LMIs of equations (2.4)-(2.5) over the parameter subset $\mathcal{P}_{s_\cap} \cup \mathcal{P}_d$. Since all three methods keep X_1 and Y_1 over the parameter subset $\mathcal{P}_{s_1} - \mathcal{P}_{s_\cap}$, the blended LPV controllers generated by the three methods are equal to the regionally designed LPV controller K_1 over the parameter subset $\mathcal{P}_{s_1} - \mathcal{P}_{s_\cap}$. Both methods I and III can, also, keep the regional LPV controller K_2 over the parameter subset $\mathcal{P}_{s_2} - \mathcal{P}_{s_\cap}$.

The disadvantage of method I is that choosing blending functions is in an *ad-hoc* manner. However, method I is the fastest to synthesize an LPV controller over the entire parameter set among the three blending methods. In method II, the blending solution matrices X_b and Y_b are guaranteed to be feasible solutions over the parameter subset $\mathcal{P}_{s_\cap}$. This method II requires solving the LMI optimization with the extra LMI constraints. In method III, optimal blending matrix functions are calculated to minimize the induced $\mathcal{L}_2$ norm γ over the parameter set $\mathcal{P}_{s_\cap}$, based on basis functions defined by a controller designer. It is unknown how the basis functions affect the blending matrix functions and the LPV control design.

4. Quasi-LPV Model of F-16 Longitudinal Axes. In this section, a quasi-LPV model of F-16 longitudinal axes is presented. The full nonlinear equations of an F-16A aircraft are taken from Ref. [1]. The nonlinear equations of F-16 longitudinal axes [1] are

$$\begin{aligned}\dot{V} &= \frac{\overline{q}S\cos\alpha}{m}[C_X(\alpha,\delta_e) + \frac{\bar{c}}{2V}C_{X_q}(\alpha)q] + \frac{\overline{q}S\sin\alpha}{m}[C_Z(\alpha,\delta_e) + \frac{\bar{c}}{2V}C_{Z_q}(\alpha)q] \\ &\quad - g\sin(\theta-\alpha) + T\cos\alpha, \qquad (4.1)\\ \dot{\alpha} &= \frac{g\cos(\theta-\alpha)}{V} - \frac{\sin\alpha}{mV\cos\beta}T + [1 + \frac{\overline{q}S\bar{c}}{2mV^2}(C_{Z_q}(\alpha)\cos\alpha - C_{X_q}(\alpha)\sin\alpha)]q \\ &\quad + \frac{\overline{q}S}{V_t}[C_Z(\alpha,\delta_e)\cos\alpha - C_X(\alpha,\delta_e)\sin\alpha], \qquad (4.2)\\ \dot{q} &= \frac{\overline{q}S\bar{c}}{2I_{yy}V}(\bar{c}C_{m_q}(\alpha) + \Delta C_{Z_q}(\alpha))q + \frac{\overline{q}S\bar{c}}{I_{yy}}(C_{m_o}(\alpha,\delta_e) + \frac{\Delta}{\bar{c}}C_Z(\alpha)), \qquad (4.3)\\ \dot{\theta} &= q. \qquad (4.4)\end{aligned}$$

Velocity (V, ft/sec), angle of attack (α, rad), pitch rate (q, rad/sec), and pitch angle (θ, rad) are the state variables and thrust (T, lb) and elevator deflection (δ_e, rad) are the control variables. The aerodynamic coefficients are lookup tables based on wind-tunnel data from NASA-Langley wind-tunnel tests on an F-16 aircraft scaled model [16]. The aerodynamic data were valid for a speed range of $100 \le V \le 900$ ft/sec, an angle of attack range of -10° $\le \alpha \le$ 45°, and an altitude range of $5000 \le h \le 40000$ ft. These three parameters are scheduling parameters in the quasi-LPV model derived for the F-16 longitudinal axes. Note that V and α are both scheduling parameters and states and h is a scheduling parameter which enters implicitly into the nonlinear dynamics.

Unfortunately, the control variable δ_e does not enter affinely in equations (4.1)-(4.3). To derive a quasi-LPV model of F-16 longitudinal axes, it is necessary that all controls be in affine form. This is achieved by transforming (δ_e, T) into synthetic inputs $u_s = [u_1 \;\; u_2]^T$. For details of the transformation, readers are referred to Ref. [14]. For the F-16 quasi-LPV model, $\cos\theta$ and $\sin\theta$ are linearized about a trim value θ_o. After tedious algebraic manipulations, equations (4.1)-(4.4) are rewritten as

$$\begin{aligned}\dot{x} &= A(V,\alpha,h)x + M(V,\alpha,h)u_s + f(V,\alpha,h), \qquad (4.5)\\ x &\equiv [V \;\; \alpha \;\; q \;\; \theta-\theta_o]^T,\end{aligned}$$

where the elements of matrices $A \in \mathcal{R}^{4\times4}$, $M \in \mathcal{R}^{4\times2}$, and $f \in \mathcal{R}^{4\times1}$ are written in Appendix A.

Using the function substitution method [18, 19], the nonlinear function $f(V,\alpha,h)$ can be decomposed into quasi-linear functions $G(V,\alpha,h)[V-V_o \;\; \alpha-\alpha_o]^T$ where G is in $\mathcal{R}^{4\times2}$. Thus, a quasi-LPV model of F-16 aircraft longitudinal axes is provided. The details of function substitution are written in Appendix B. To compare simulation results of the nonlinear and the quasi-LPV model of the F-16 aircraft dynamics, several time sets of inputs T and δ_e are pre-defined. In this paper, one example of time simulations is presented for space limitation. For example, inputs are set as

$$\delta_e = \delta_{eo}, \qquad (4.6)$$

$$T = \begin{cases} T_o \text{ lb}, & 0 \le t \le 1,\ 11 \le t \\ T_o - 2000 \text{ lb}, & 1 \le t \le 11 \text{ sec}, \end{cases} \qquad (4.7)$$

where δ_{eo} and T_o is a trim value. The time simulation results in Figure 4.1 show that the time responses

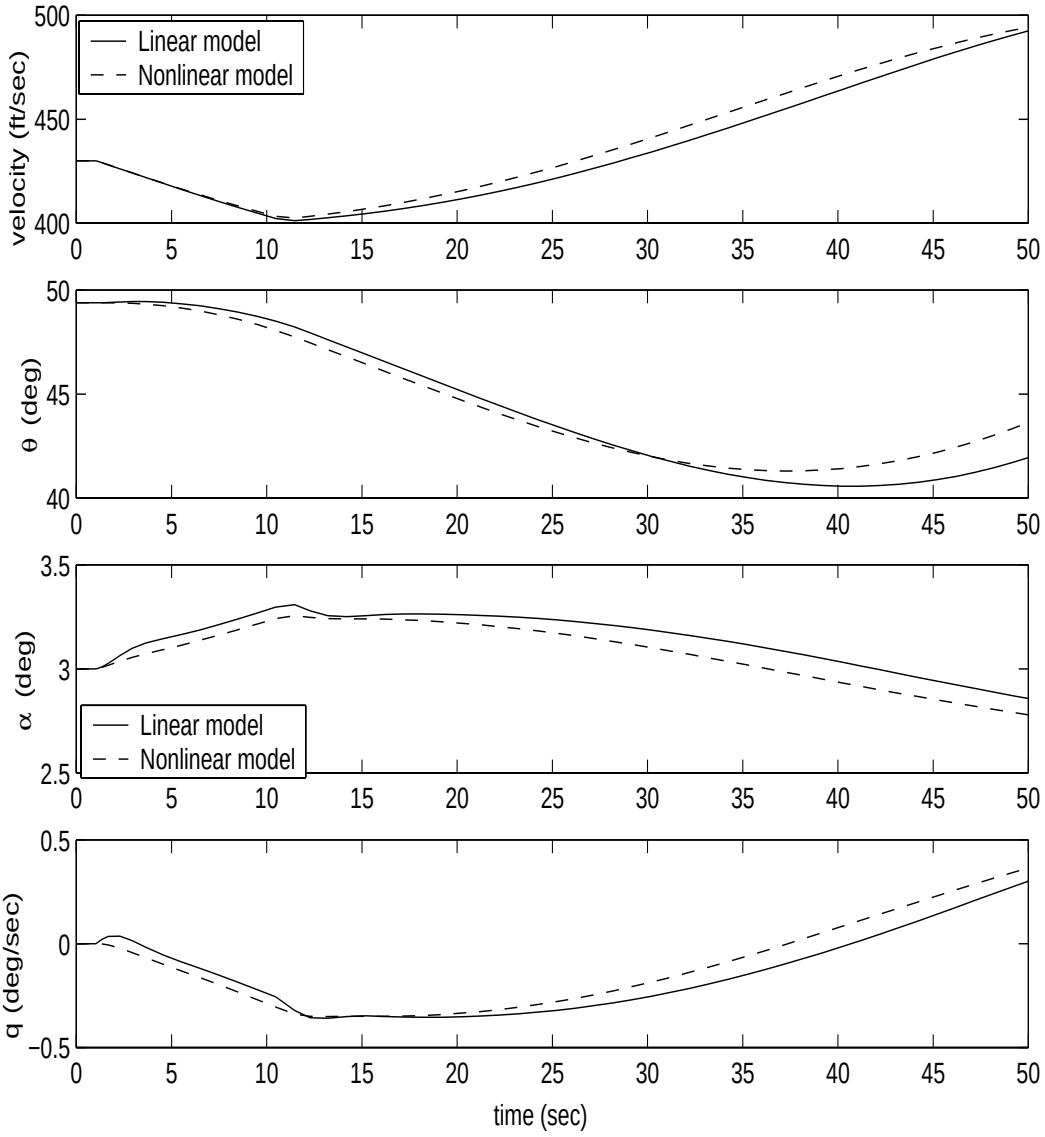

FIG. 4.1. *Nonlinear vs. quasi-LPV model simulations*

of the quasi-LPV and nonlinear models are almost matched to each other. Note that the quasi-LPV model provided by the function substitution method may change depending on which one trim point is selected. It is unknown how this affects the quasi-LPV model or the LPV control design.

5. LPV Control Problem Formulation.

5.1. Control Design Objectives and Weighting Functions. A formulation of the LPV control synthesis of the F-16 longitudinal axes is presented in this section. The primary control objective for the F-16 longitudinal flight controller is to track velocity and flight path angle commands within 1 ft/sec and 0.6° error range in steady-state conditions.

Velocity and flight path angle tracking problems can be formulated as model matching problems in the LPV control synthesis. In this paper, we consider the F-16 aircraft as an unmanned aircraft. The ideal

transfer function from the flight path angle command to the flight path angle measurement is modeled as a second order system, $\frac{0.426(s+1.5)}{\mathbf{s}^2+1.6\mathbf{s}+0.64}$ with 0.8 rad/sec bandwidth and a right hand zero at -1.5 rad/sec. For the velocity tracking problem, the ideal transfer function from the velocity command to the velocity measurement is modeled as the second order system $\frac{0.16}{\mathbf{s}^2+0.8\mathbf{s}+0.16}$ with 0.4 rad/sec natural frequency and critical damping.

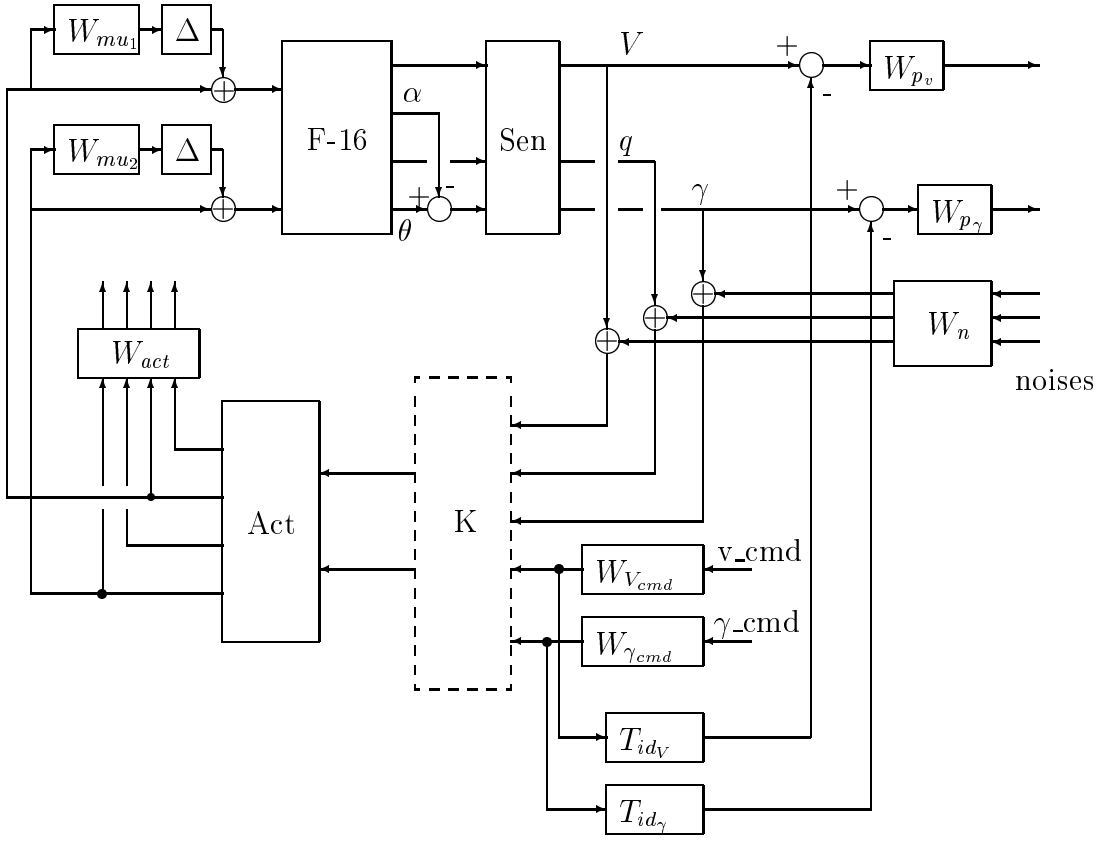

FIG. 5.1. *Interconnection structure for the model matching problems.*

A block diagram of the interconnection structure for synthesizing an LPV controller for the F-16 longitudinal axes is shown in Figure 5.1. The velocity, angle rate and angle sensors are modeled as the first-order low pass filters $\frac{50}{\mathbf{s}+50}$, $\frac{60}{\mathbf{s}+60}$, and $\frac{10}{\mathbf{s}+10}$ (see Ref. [1, 16]). In the LPV controller synthesis models, the sensor models shown in Figure 5.1 are approximated as:

$$\text{Sen} = \text{diag}([1, 1, \frac{10}{\mathbf{s}+10}]), \tag{5.1}$$

since the interesting frequency range for LPV control synthesis is less than 10 rad/sec. The reduced order sensor models help to reduce the overall state order of an LPV controller, since the state order of an LPV controller is same as that of the augmented open-loop system. The elevator actuator is modeled as the first-order lag filter $\frac{20}{\mathbf{s}+20}$ and its rate limit is defined as $\pm$ 60 deg/sec in Ref. [1, 16]. Since the F-16 is a fighter aircraft, we estimated the engine model as the first-order lag filter $\frac{4}{\mathbf{s}+4}$ which allows fast responses in engine dynamics. The thrust rate limit is taken to be 10000 lb/sec. In the block diagram in Figure 5.1, the actuator rate and actuator models are:

$$\text{Act} = \text{diag}([\frac{20\mathbf{s}}{\mathbf{s}+20}, \frac{20}{\mathbf{s}+20}, \frac{4\mathbf{s}}{\mathbf{s}+4}, \frac{4}{\mathbf{s}+4}]). \tag{5.2}$$

The performance weighting functions are chosen based on the desired performance objectives. The performance weighting function of flight path angle W_{p_γ}, $\frac{100(\mathtt{s}/100+1)^2}{(\mathtt{s}/0.6+1)^2}$, is derived based on the performance objective to keep a γ tracking error less than 0.6° for 1 radian command in steady state flight. Since the bandwidth of the ideal model from the flight path angle command to the flight path angle measurement is 0.8 rad/sec, the roll off frequency of the weighting function is chosen as 0.6 rad/sec to specify the tracking error less than 0.6° at the low frequency region (< 0.6 rad/sec). The performance weighting function for the velocity, W_{p_v}, $\frac{\mathtt{s}/200+1}{\mathtt{s}+1}$, is derived to track velocity commands within 1 ft/sec error range in steady state flight. The unmodeled dynamics are included in the multiplicative uncertainty models, W_{mu_1} and W_{mu_2}. The uncertainty weighting functions are rolled up in the mid-frequency range in order to limit the bandwidth of the LPV controllers. The multiplicative uncertainty weight functions are set as

$$W_{mu1} = \frac{0.01(\mathtt{s}/0.35+1)}{\mathtt{s}/80+1},$$
$$W_{mu2} = \frac{0.01(\mathtt{s}/0.2+1)}{\mathtt{s}/50+1}.$$

The sensor noise models are taken as constant across frequency to reduce the state order of the LPV controllers. The velocity, angle, and angle rate sensor noises are modeled as white noises with amplitudes of 0.8 ft/sec, 0.1°, and 0.6 deg/sec, respectively.

To solve LMI equations (2.4)-(2.6), the basis function sets need to be defined for X and Y. There is no analytical method to choose the best basis function set. Most often the basis functions used are power series[7], Legendre polynomials[10], or affine functions of scheduling parameters [9]. Here, the basis function set for $X(\rho)$ and $Y(\rho)$ is chosen as the first order power series $\{1,\ \rho\}$ of the scheduling parameter of velocity to reduce the computation time in the LPV control synthesis. Note that the basis functions of X and Y do not have to be same.

5.2. Blending Two Controllers. In this section, synthesizing an LPV controller for the F-16 longitudinal axes using the blending approach is demonstrated. To apply the blending approach for control of the F-16, the entire parameter set (the flight envelope) is partitioned into two subsets: high and low altitude regions. Parameter subsets are:

$$\begin{aligned}
\mathcal{P}_1 &\equiv \{(V,\alpha,h)|100 \le V \le 900\,\text{ft/sec}, \quad -10 \le \alpha < 45^\circ, \quad 5000 \le h < 30000\,ft\},\\
\mathcal{P}_2 &\equiv \{(V,\alpha,h)|100 \le V \le 900\,\text{ft/sec}, \quad -10 \le \alpha < 45^\circ, \quad 10000 < h \le 40000\,\text{ft}\},\\
\mathcal{P}_\cap &\equiv \mathcal{P}_1 \cap \mathcal{P}_2.
\end{aligned} \tag{5.3}$$

To use methods I and II, blending functions are required over the parameter subset $\mathcal{P}_\cap$, which are satisfied with the boundary conditions of equations (3.5)-(3.7). Blending functions $b_1(h)$ and $b_2(h)$ are chosen as:

$$b_1(h) = \begin{cases} 1, & h \le 10000\,ft,\\ 0.5[1+\cos(\frac{h-10000}{20000}\pi)], & 10000 < h < 30000\,ft,\\ 0, & 30000\,ft \le h, \end{cases} \tag{5.4}$$

and

$$b_1(h) + b_2(h) = 1. \tag{5.5}$$

Using the blending functions, the solution matrices X_i and Y_i are blended across the parameter subset $\mathcal{P}_\cap$ as:

$$X_b(V,\alpha,h) = b_1(h)X_1(V,\alpha) + b_2(h)X_2(V,\alpha), \tag{5.6}$$

$$Y_b(V,\alpha,h) = b_1(h)Y_1(V,\alpha) + b_2(h)Y_2(V,\alpha). \tag{5.7}$$

Using method I, an LPV controller K_I is constructed with the solution matrices X_b and Y_b using equations (2.8)-(2.11) over the entire parameter set $\mathcal{P}_1 \cup \mathcal{P}_2$.

Using the blending functions in equations (5.4)-(5.5) and the solution matrices X_1 and Y_1 over the parameter subset $\mathcal{P}_1$, the solution matrices X_2 and Y_2 are determined solving the LMI optimization over the parameter set $\mathcal{P}_2$ with the extra LMIs of equations (3.14)-(3.15) described in method II. An LPV controller K_{II} is constructed based on the calculated blended matrices X_b and Y_b using equations (2.8)-(2.11) over the entire parameter set.

To blend solution matrices $X_i(V,\alpha)$ and $Y_i(V,\alpha)$ calculated over each parameter subset, the basis functions for blending matrix functions of equations (3.18) and (3.19) are required to use method III. In this paper, the basis function sets are chosen as $\{g_0, \quad g_1\}$ for X_{b_1} and Y_{b_1}, and as $\{h_0, \quad h_1\}$ for X_{b_2} and Y_{b_2}, respectively.

$$g_0(h) = \begin{cases} 1, & h \le 10000\ ft, \\ 0.5[1+\cos(\frac{h-10000}{20000}\pi)], & 10000 < h < 30000\ ft, \\ 0, & 30000\ ft \le h, \end{cases} \tag{5.8}$$

$$g_1(h) = \begin{cases} 0, & h \le 10000\ ft, \\ 0.15[1+\cos(\frac{h-20000}{10000}\pi)], & 10000 < h < 30000\ ft, \\ 0, & 30000\ ft \le h, \end{cases} \tag{5.9}$$

$$h_0(h) = 1 - g_0(h), \quad h_1(h) = -g_1(h). \tag{5.10}$$

Note that it is not necessary to choose the same basis functions for X_{b_i} and Y_{b_i}. From the solution of the LMI optimization of equation (3.21), the matrices $X_b(V,\alpha,h)$ and $Y_b(V,\alpha,h)$ are calculated using equations (3.16)-(3.19). An LPV controller K_{III} is constructed from the matrices $X_b(V,\alpha,h)$ and $Y_b(V,\alpha,h)$ using equations (2.8)-(2.11) over the entire parameter set.

For comparison, an LPV controller K_{tot} is constructed with solution matrices X and Y over the entire parameter set using the conventional LPV controller synthesis approach. It takes approximately 43 hours on 933 MHz PIII machine running Linux. Using the blending methods I, II, and III, it takes approximately 22, 25, and 30 hours on the same machine, respectively. The computation time to synthesize the LPV controller for the F-16 longitudinal axes is reduced using the blending approaches.

6. Nonlinear Simulations. The 12 state nonlinear F-16 aircraft dynamics [1] with the synthesized LPV controllers, K_1, K_2, K_{tot}, K_I, K_{II}, and K_{III}, are simulated to compare their time simulations in this section. Recall that the LPV controllers K_1 and K_2 are constructed over parameter subsets $\mathcal{P}_1$ and $\mathcal{P}_2$, respectively. The LPV controller K_{tot} is synthesized over the entire parameter set, using the conventional LPV control synthesis methodology. The LPV controllers K_I, K_{II}, and K_{III} are the blended controller using the blending methods I, II, and III, respectively. In simulations, the LPV controller is implemented

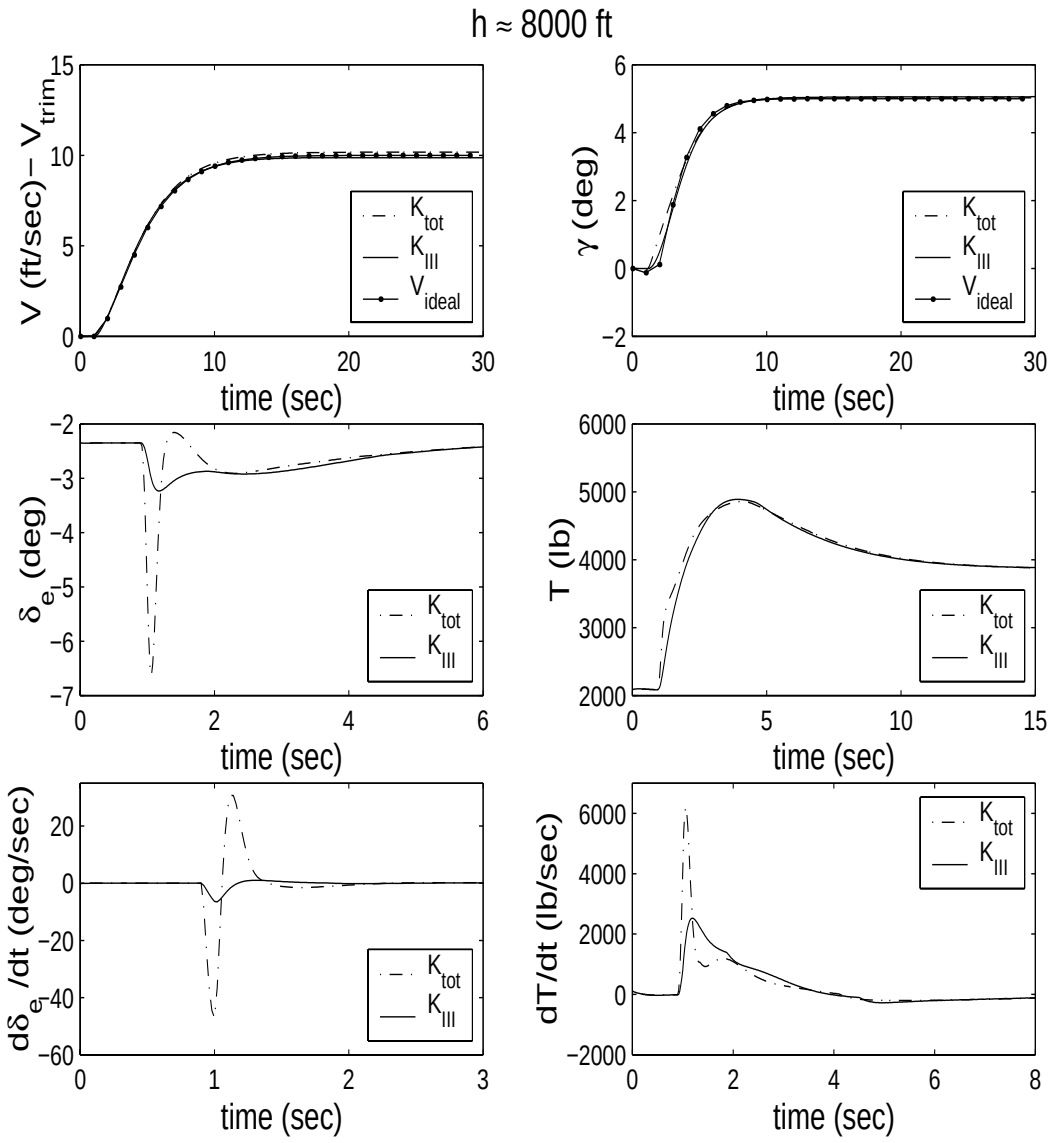

FIG. 6.1. *Time simulations with the LPV controllers around 8000 ft altitude.*

using linear interpolation at the current values of the scheduling parameters between the grid point solutions. The full state models of actuators and sensors are included in the nonlinear F-16 aircraft simulations.

Using these LPV controllers, the velocity and γ step responses are simulated around 8000 ft and 32000 ft altitude, respectively. The step input sizes are a 10 ft/sec velocity command and a 5° γ command at 1 sec. The simulation results in Figure 6.1 show that all velocity and γ measurements match the ideal responses within ± 0.25 ft/sec and 0.06° tracking error. It is observed that these LPV controllers achieve the desired performance objectives.

The LPV controllers K_1, K_I, K_{II}, and K_{III} are exactly equal to each other over the parameter subset $\mathcal{P}_1 - \mathcal{P}_\cap$, since the blending methods I, II, and III keep the regional LPV controller K_1 over the parameter subset $\mathcal{P}_1 - \mathcal{P}_\cap$. The step responses of velocity and γ with the LPV controller K_{III} in Figure 6.1 represent the step responses with the LPV controllers K_1, K_I, and K_{II} in the simulations around 8000 ft altitude.

The actuator deflections and their rates of the time simulations are shown in Figure 6.1. It is noted that the blended LPV controller K_{III} uses smaller actuator deflections and their rates than the LPV controller K_{tot} does to achieve the performance objectives.

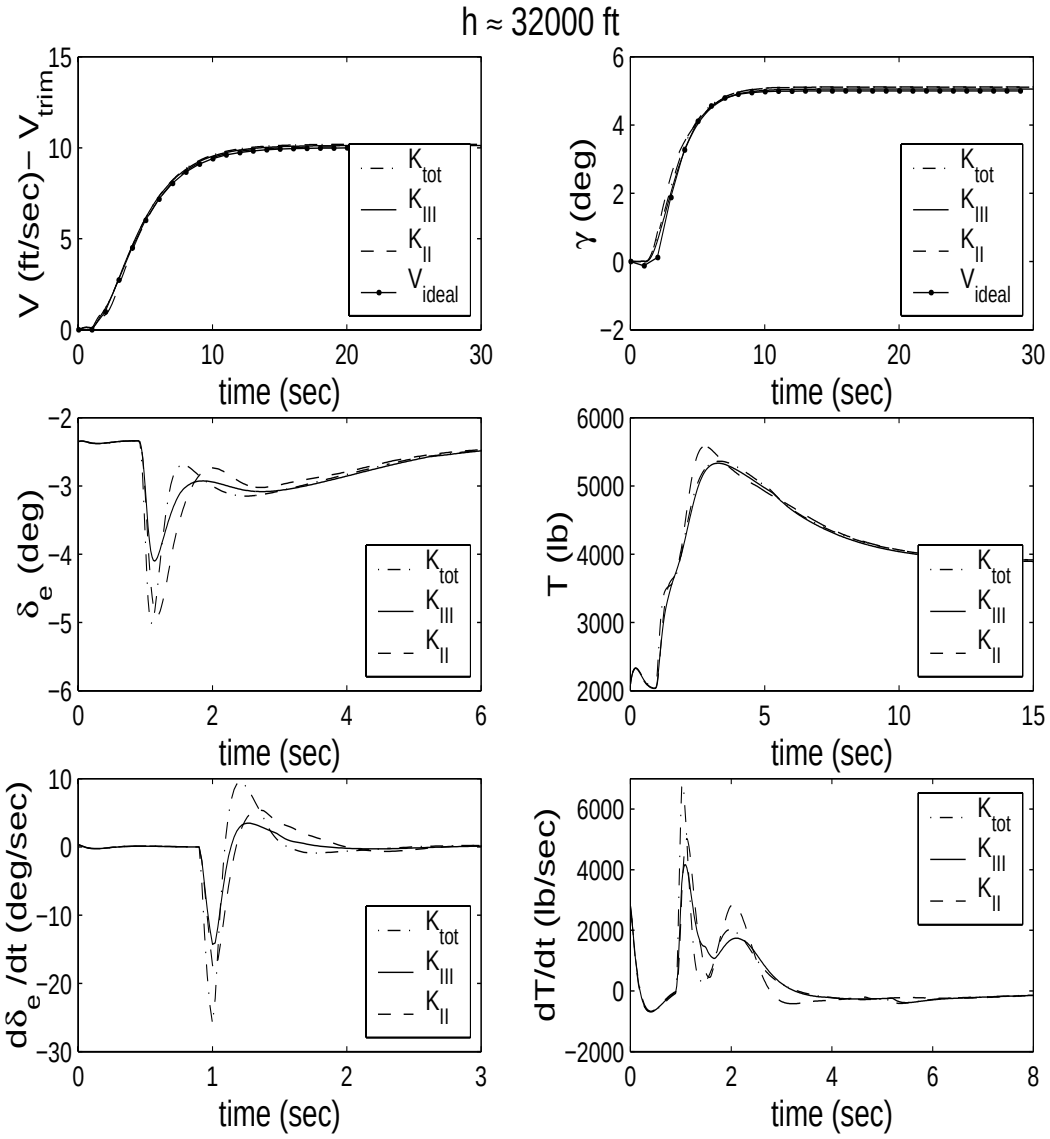

FIG. 6.2. *Time simulations with the LPV controllers around 32000 ft altitude.*

The LPV controllers K_2, K_I, and K_{III} are exactly equal to each other over the parameter subset $\mathcal{P}_2 - \mathcal{P}_\cap$. The blended LPV controller K_{II} is different from K_2 over the parameter subset $\mathcal{P}_2 - \mathcal{P}_\cap$, since in the method II, the blended controller is constructed solving the LMI optimization of equations (2.3)-(2.6) with the extra LMI constraints of equations (3.14)-(3.15). The step responses with the LPV controllers K_{tot}, K_{III}, and K_{II} are shown in Figure 6.2. It is observed that these LPV controllers achieve the desired performance objectives over the parameter set $\mathcal{P}_2 - \mathcal{P}_\cap$. The simulation results show that the LPV controller K_{tot} uses the largest actuator deflections and their rates to achieve the performance objectives.

For comparison, there is simulated one of candidate maneuvers that the F-16 aircraft flies from 15000 ft

to 32000 ft across the parameter subset $\mathcal{P}_\cap$, using 20 and 10 ft/sec velocity step and 10° γ step commands. Velocity, flight path angle, altitude, and angle of attack time responses with the LPV controllers K_{tot}, K_{III}, K_{II}, and K_I are shown in Figure 6.3. All the LPV controllers can achieve the performance objectives across the parameter subset $\mathcal{P}_\cap$. It is noticed that the velocity tracking performance with the blended controllers is slightly better than the LPV controller K_{tot} designed over the entire parameter set $\mathcal{P}_1 \cup \mathcal{P}_2$ using the conventional LPV controller synthesis methodology. The actuator deflections and their rates with the LPV controllers are shown in Figure 6.4. The simulation results show that the blended controllers use much smaller actuator deflections to track the velocity and γ commands.

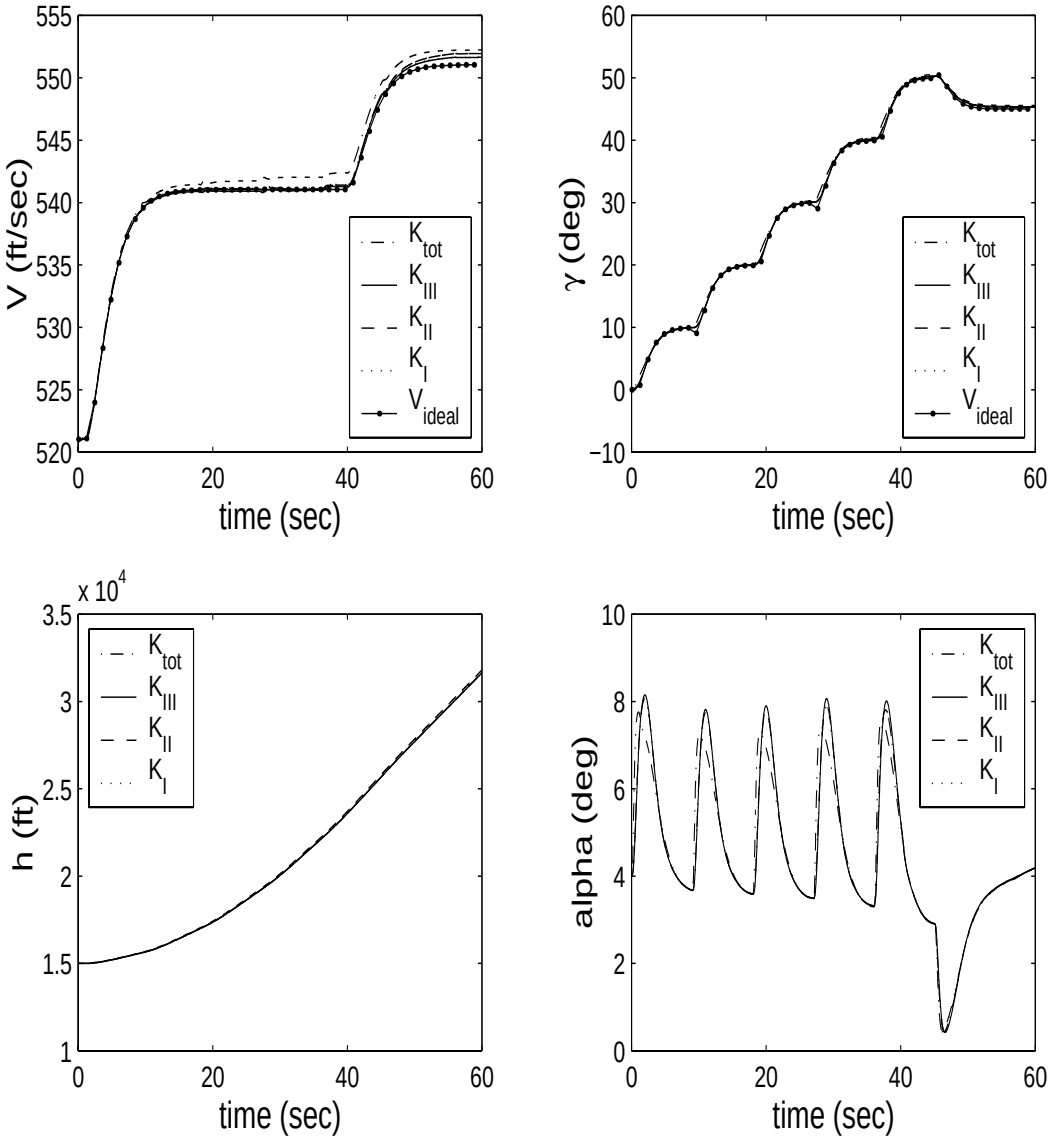

FIG. 6.3. *Time simulations with the LPV controllers for the candidate maneuver.*

Sensor noises are integrated into the F-16 aircraft simulations for the same situation of flying the F-16 aircraft from 15000 ft to 32000 ft. Sensor noises for pitch rate, velocity and pitch angle are set as white noises with ±0.5 deg/sec, ± 0.8 ft/sec, and ±0.1° amplitudes. The simulation results are omitted for space

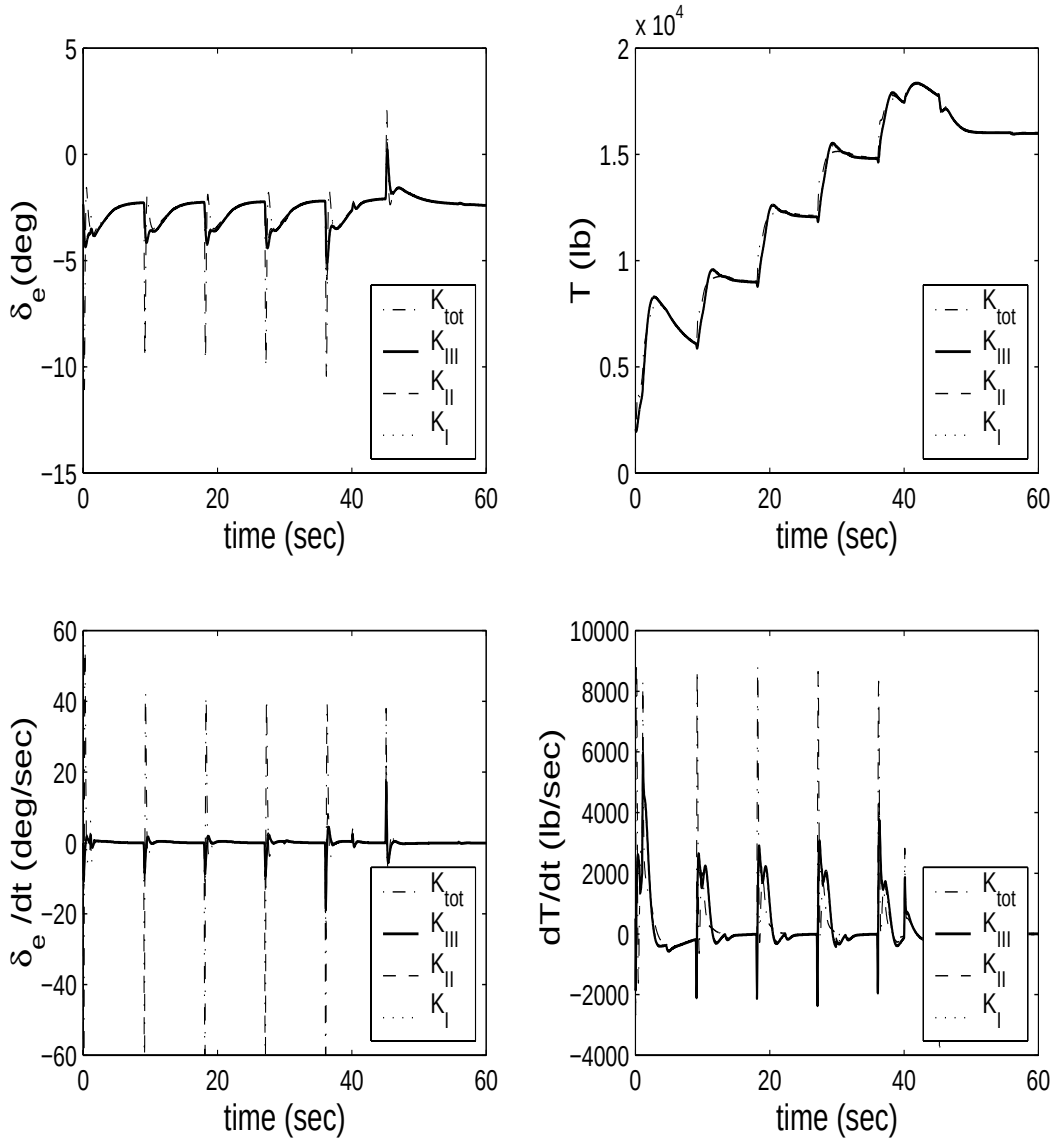

FIG. 6.4. *Actuator time responses with the LPV controllers for the candidate maneuver.*

limitations. The LPV controllers K_{tot}, K_{III}, K_{II}, and K_I stabilize the F-16 aircraft with the sensor noises and achieve tracking performance objectives over the scheduling parameter variations. The thrust signal and its rate do not exceed their limits: $T < 19000$ lb and $|\frac{dT}{dt}| < 10000$ lb/sec. Also, the elevator actuator and its rates do not exceed their limits: $|\delta_e| < 25^\circ$ and $|\frac{d\delta_e}{dt}| < 60$ deg/sec. The blended controllers K_{III} and K_I can preserve the performance level of the regional LPV controllers K_1 and K_2 over each parameter subset $\mathcal{P}_1$ and $\mathcal{P}_2$.

Note that method I requires the slow parameter-varying blending functions. In this example, the parameter intersection range is wide enough to provide the slow-varying blending functions for method I. When the parameter intersection space is narrow, method III is appropriate to blend two LPV controllers over the parameter intersection space.

7. Summary and Discussion. In this paper, the methodologies of blending LPV controllers are discussed to preserve the performance level over each parameter subset and to reduce computation time to synthesize an LPV controller over the entire parameter set. The blending approaches are to design each LPV controller for the set of a small number of scheduling parameters over the parameter subsets and blend all controllers scheduled on the entire scheduling parameters using the blending functions.

The quasi-LPV model of the F-16 longitudinal axes is provided by a function substitution method over the entire flight envelope to facilitate synthesis of an LPV controller. The two LPV controllers of the F-16 longitudinal axes are synthesized as functions of velocity and angle of attack at two regions: low and high altitudes, respectively. The two LPV controllers are blended into a single LPV controller as functions of velocity, angle of attack, and altitude over the entire flight envelope, using the three blending approaches. It is noted from the nonlinear time simulations that the blended controllers achieve better performance than the LPV controller constructed using the conventional LPV synthesis methodology. The blended controllers constructed using methods I, II, and III achieve the performance objectives and stabilize the closed-loop system of the F-16 aircraft with sensor noises.

Acknowledgements. The technical monitor was Dr. Christine Belcastro at NASA Langley Research Center.

REFERENCES

[1] B. Stevens and F. Lewis, *Aircraft Control and Simulation*, John Wiley and Sons Inc., 1992.

[2] F. Wu, *Control of Linear Parameter Varying Systems*, PhD thesis, Department of Mechanical Engineering, University of California, Berkeley, 1995.

[3] F. Wu, A. Packard, and G. Balas, *LPV Control Design for Pitch-Axis Missile Autopilots*, in Proceedings of the 34th Conference on Decision and Control, New Orleans, LA, 1995, pp. 188–193.

[4] G. Balas, A. Packard, J. Renfrow, C. Mullaney, and R. M'Closky, *Control of the F-14 Aircraft Lateral-Directional Axis During Powered Approach*, Journal of Guidance, Control, and Dynamics, 21 (1998), pp. 899–908.

[5] G. Balas, I. Fialho, A. Packard, J. Renfrow, and C. Mullaney, *On the Design of LPV Controllers for the F-14 Aircraft Lateral-Directional Axis During Powered Approach*, in Proceedings of the American Control Conference, Albuquerque, NM, 1997, pp. 123–127.

[6] G. Becker, *Quadratic Stability and Performance of Linear Parameter Dependent Systems*, PhD thesis, Department of Engineering, University of California, Berkeley, 1993.

[7] ——, *Parameter-Dependent Control of an Under-Actuated Mechanical System*, in Proceedings of the 34th IEEE Conference on Decision and Control, New Orieans, LA, 1995, pp. 543–548.

[8] G. Wolodkin, G. Balas, and W. Garrard, *Application to Parameter Dependent Robust Control Synthesis to Turbofan Engines*, in AIAA, Aerospace Sciences Meeting and Exhibit, AIAA-98-0973, Reno, NV, 1998.

[9] G. Wood, *Control of Parameter-Dependent Mechanical Systems*, PhD thesis, Department of Engineering, University of Cambridge, 1995.

[10] J. Primbs, *Nonlinear Optimal Control: A Receding Horizon Approach*, PhD thesis, Department of Engineering, University of Cambridge, 1999.

[11] J. Shamma, *Gain-Scheduled Missile Autopilot Design Using Linear Parameter Varying Transformations*, Journal of Guidance, Control, and Dynamics, 16 (1993), pp. 256–261.

[12] J. Shamma and M. Athans, *Analysis of Gain Scheduled Control for Nonlinear Plants*, IEEE Transactions on Automatic Control, 35 (1990), pp. 898–907.

[13] ——, *Guaranteed Properties of Gain Scheduled Control for Linear Parameter-Varying Plants*, Automatica, 35 (1991), pp. 559–564.

[14] J-Y. Shin, *Worst-case Analysis and Linear Parameter Varying Control of Aerospace System*, PhD thesis, University of Minnesota, 2000.

[15] L. Lee, *Identification and Robust Control of Linear Parameter-Varying Systems*, PhD thesis, Department of Mechanical Engineering, University of California, Berkeley, 1997.

[16] L. Nguyen, M. Ogburn, W. Gilbert, K. Kibler, P. Brown, and P. Deal, *Simulator Study of Stall/Post-Stall Characteristics of a Fighter Airplane with Relaxed Longitudinal Static Stability*, tech. report, NASA Scientific and Technical Information Branch, 1979. NASA Technical Paper 1538.

[17] P. Apkarian and R. Adams, *Advanced Gain-Scheduling Techniques for Uncertain Systems*, IEEE Transactions on Control Systems Technology, 6 (1998), pp. 21–32.

[18] W. Tan, *Applications of Linear Parameter-Varying Control Theory*, Master's thesis, Department of Mechanical Engineering, University of California at Berkeley, 1997.

[19] W. Tan, A. Packard, and G. Balas, *Quasi-LPV Modeling and LPV Control of a Generic Missile*, in Proceedings of the American Control Conference, Chicago, IL, 2000, pp. 3692–3696.

Appendix A. Nonlinear Equations of F-16 Longitudinal Axes. From nonlinear equations (4.1)-(4.4), the nonlinear equations of the F-16 longitudinal axes are rewritten as follows:

$$\begin{bmatrix} \dot{V} \\ \dot{\alpha} \\ \dot{q} \\ \dot{\theta} \end{bmatrix} = \begin{bmatrix} A_{11}(V,\alpha) & A_{12}(V,\alpha,h) \\ A_{21}(V,\alpha) & A_{22}(V,\alpha,h) \end{bmatrix} \begin{bmatrix} V \\ \alpha \\ q \\ \theta - \theta_o \end{bmatrix} + M(V,\alpha,h)u_s + f(V,\alpha), \tag{A.1}$$

where

$$A_{11} = A_{21} = \begin{bmatrix} 0 & 0 \\ 0 & 0 \end{bmatrix},$$

$$\begin{aligned} A_{12}(1,1) &= \frac{\overline{q}S\bar{c}}{2mV}(C_{X_q}(\alpha)\cos\alpha + C_{Z_q}(\alpha)\sin\alpha), \\ A_{12}(1,2) &= g(-\cos\alpha\cos\theta_o - \sin\alpha\sin\theta_o), \\ A_{12}(2,1) &= 1 + \frac{\overline{q}S\bar{c}}{2mV^2}(-C_{X_q}(\alpha)\sin\alpha + C_{Z_q}(\alpha)\cos\alpha), \\ A_{12}(2,2) &= \frac{g}{V}(\sin\alpha\cos\theta_o - \cos\alpha\sin\theta_o), \end{aligned}$$

$$A_{22} = \begin{bmatrix} \frac{\overline{q}S\bar{c}}{2VI_{yy}}(\bar{c}C_{m_q}(\alpha) + \Delta C_{Z_q}(\alpha)) & 0 \\ 1 & 0 \end{bmatrix},$$

$$f = \begin{bmatrix} \frac{\overline{q}S}{m}C_Z(\alpha)\sin\alpha + g(-\cos\alpha\sin\theta_o + \sin\alpha\cos\theta_o) \\ \frac{\overline{q}S}{mV}C_Z(\alpha)\cos\alpha + \frac{g}{V}(\sin\alpha\sin\theta_o + \cos\alpha\cos\theta_o) \\ \frac{\overline{q}S}{I_{yy}}\Delta C_Z(\alpha) \\ 0 \end{bmatrix}.$$

The gain matrix M is constructed as lookup tables and u_s are synthetic inputs. The term of $M(V,\alpha,h)u_s$ can represent the following terms:

$$M(V,\alpha,h)u_s(V,\alpha,\delta_e,T) \approx \begin{bmatrix} \frac{\bar{q}S}{m}[\bar{C}_{Z_e}\delta_e \sin\alpha + C_X(\alpha,\delta_e)\cos\alpha] + \frac{\cos\alpha}{m}T \\ \frac{\bar{q}S}{mV}[\bar{C}_{Z_e}\delta_e \cos\alpha - C_X(\alpha,\delta_e)\sin\alpha] - \frac{\sin\alpha}{mV}T \\ \frac{\bar{q}S\bar{c}}{I_{yy}}C_M(\alpha,\delta_e) + \frac{\bar{q}S}{I_{yy}}\Delta\bar{C}_{Z_e}\delta_e \\ 0 \end{bmatrix}.$$

The detailed methods to determine M and synthetic inputs u_s are available in Ref. [14]. The synthetic inputs can vary in the range of $-1 \le u_1 \le 1$ and $0 \le u_2 \le 1$. The units of u_1 and u_2 are 25° and 19000 lb, respectively.

Appendix B. Decomposition. Set the state variables in a quasi-LPV model of the F-16 aircraft dynamics as $V - V_o$, $\alpha - \alpha_o$, $q - q_o$ and $\theta - \theta_o$, where V_o, α_o, q_o and θ_o represent a trim point. Then, equation (A.1) is rewritten as

$$\begin{bmatrix} \dot{\xi}_1 \\ \dot{\xi}_2 \end{bmatrix} = F(z) + \begin{bmatrix} A_{11}(z) & A_{12}(z) \\ A_{21}(z) & A_{22}(z) \end{bmatrix} \begin{bmatrix} \xi_1 \\ \xi_2 \end{bmatrix} + \begin{bmatrix} B_1(z) \\ B_2(z) \end{bmatrix} \tilde{u}, \tag{B.1}$$

where

$$F(z) = f(z) + \begin{bmatrix} A_{11}(z) & A_{12}(z) \\ A_{21}(z) & A_{22}(z) \end{bmatrix} \begin{bmatrix} z_o \\ w_o \end{bmatrix} + \begin{bmatrix} B_1(z) \\ B_2(z) \end{bmatrix} u_o,$$

$$\xi_1 = z - z_o, \quad \xi_2 = w - w_o, \quad \tilde{u} = u_s - u_o, \tag{B.2}$$

and

$$z = [V \;\; \alpha]^T, \qquad w = [q \;\; \theta]^T. \tag{B.3}$$

To provide a quasi-LPV model of F-16 aircraft dynamics from equation (B.1), the term $F(z)$ should be decomposed into linear parameter varying functions written as

$$F(z) = F(z_o + \xi_1) = \begin{bmatrix} g_z(z_o + \xi_1) \\ g_w(z_o + \xi_1) \end{bmatrix} \xi_1, \tag{B.4}$$

where $g_z \in \mathcal{R}^{2\times 2}$ and $g_w \in \mathcal{R}^{2\times 2}$. There are an infinite number of possible solutions of g_z and g_w to satisfy equation (B.4). To determine functions g_z and g_w, more constraints are required. In this paper, the variation of g_z and g_w over the entire flight envelope is minimized. With these constraints, an optimization problem is formulated to determine g_z and g_w. For example, to determine the first row of g_z, an optimization problem is follows:

$$\min_{g_{z_{11}} \in \mathcal{R}, g_{z_{12}} \in \mathcal{R}} \epsilon, \tag{B.5}$$

subject to

$$F_1(z_o + \xi_1) = [g_{z_{11}}(z_o + \xi_1) \;\; g_{z_{12}}(z_o + \xi_1)]\xi_1 \tag{B.6}$$

$$\left|\frac{\partial^2 g_{z_{11}}(z_o + \xi_1)}{\partial \xi_1^2}\right| \le \epsilon, \quad \left|\frac{\partial^2 g_{z_{12}}(z_o + \xi_1)}{\partial \xi_1^2}\right| \le \epsilon,$$

where F_1 is the first row of F. To make the optimization problem of equation (B.5) computationally tractable, the continuous constraints are evaluated at grid points over the parameter set. Thus, the matrix g_z can be determined at every grid point of ξ_1. Using solutions of the optimization for g_z and g_w, a quasi-LPV model of F-16 longitudinal axes is written as:

$$\begin{bmatrix} \dot{V} \\ \dot{\alpha} \\ \dot{q} \\ \dot{\theta} \end{bmatrix} = \begin{bmatrix} A_{11}(V,\alpha) + g_z(V,\alpha) & A_{12}(V,\alpha,h) \\ A_{21}(V,\alpha) + g_w(V,\alpha) & A_{22}(V,\alpha,h) \end{bmatrix} \begin{bmatrix} V - V_o \\ \alpha - \alpha_o \\ q \\ \theta - \theta_o \end{bmatrix} + M(V_t,\alpha,h)(u_s - u_{so}). \tag{B.7}$$